Passive Ranging of Tonal Sources in Shallow Water Using the Waveguide Invariant

by

Andrew Young

Department of Electrical and Computer Engineering
Duke University

Date: _____

Approved:

_____
Jeffrey Krolik, Supervisor

_____
Loren Nolte

_____
William Joines

_____
Donald Bliss

Thesis submitted in partial fulfillment of
the requirements for the degree of Master of Science in the Department of
Electrical and Computer Engineering in the Graduate School
of Duke University

2017

ABSTRACT

Passive Ranging of Tonal Sources in Shallow Water Using the Waveguide Invariant

by

Andrew Young

Department of Electrical and Computer Engineering
Duke University

Date: _____

Approved:

_____
Jeffrey Krolik, Supervisor

_____
Loren Nolte

_____
William Joines

_____
Donald Bliss

An abstract of a thesis submitted in partial
fulfillment of the requirements for the degree
of Master of Science in the Department of
Electrical and Computer Engineering in the Graduate School
of Duke University

2017

Abstract

Shallow water, coastal regions with high volumes of shipping traffic provide an excellent opportunity to passively characterize the ocean acoustic propagation environment. In this paper, a hybrid maximum-likelihood method is presented for estimating the value of the waveguide invariant parameter, β, which succinctly characterizes the interference structure inherent to ducted acoustic propagation. A similar method is also presented by which the range can be estimated to a tonal source that later transits a shallow water region that has previously been characterized by β. This paper focuses solely on tonal acoustic sources, exploiting one of the defining characteristics of cargo ship emissions. The methods presented require minimal a priori environmental knowledge and relatively few assumptions regarding the acoustic sources. β is estimated through spectral analysis of the fading pattern of a received acoustic signal from a transiting cargo ship that broadcasts its GPS location through Automatic Identification System (AIS) data. Range is estimated using a similar method, but also requiring a rough source velocity estimate. Close agreement is seen between simulated results obtained using Kraken and experimental results using data from the Swellex 96 experiment, in which a shallow source was used to estimate the range to a deep source.

Contents

List of Figures

Acknowledgements

This work was funded by the Office of Naval Research as part of a Multidisciplinary University Research Initiative (MURI) on the topic of exploiting the information content of ocean noise. I would like to thank my advisor, Dr. Jeffrey Krolik, and especially Dr. Andrew Harms, who played a critical role in guiding me through my first two years of research on the waveguide invariant.

Most importantly, I would like to thank my loving wife, Jenna, for her patient and unwaivering support.

1

Introduction

1.1 Introduction to the waveguide invariant

The waveguide invariant, commonly denoted as β, is a compact, scalar parameter that characterizes the frequency- and range-varying dispersion of sound in an ocean acoustic waveguide. The waveguide invariant was first described in 1982 by the Russian scientist S.D. Chuprov, who presented the parameter in the context of the readily-observable interference structures which derive from the coherent addition of propagating modes in a ducted environment [1]. Chuprov noted that, without obtaining a multitude of precise spatially- and temporally-varying measurements of environmental parameters required to compute exact phase differences between all propagating modes, the interference structure of the total pressure field can still be obtained with great fidelity by leveraging β, even at ranges of tens of kilometers [1]. Interference structures can be observed visually by plotting the magnitude of a channel's frequency response as a function of source-receiver range, as shown in Figure 1.1. With an appropriate offset to account for source transmit level, this can be viewed as a plot of the measured, received spectral intensity of a radiated

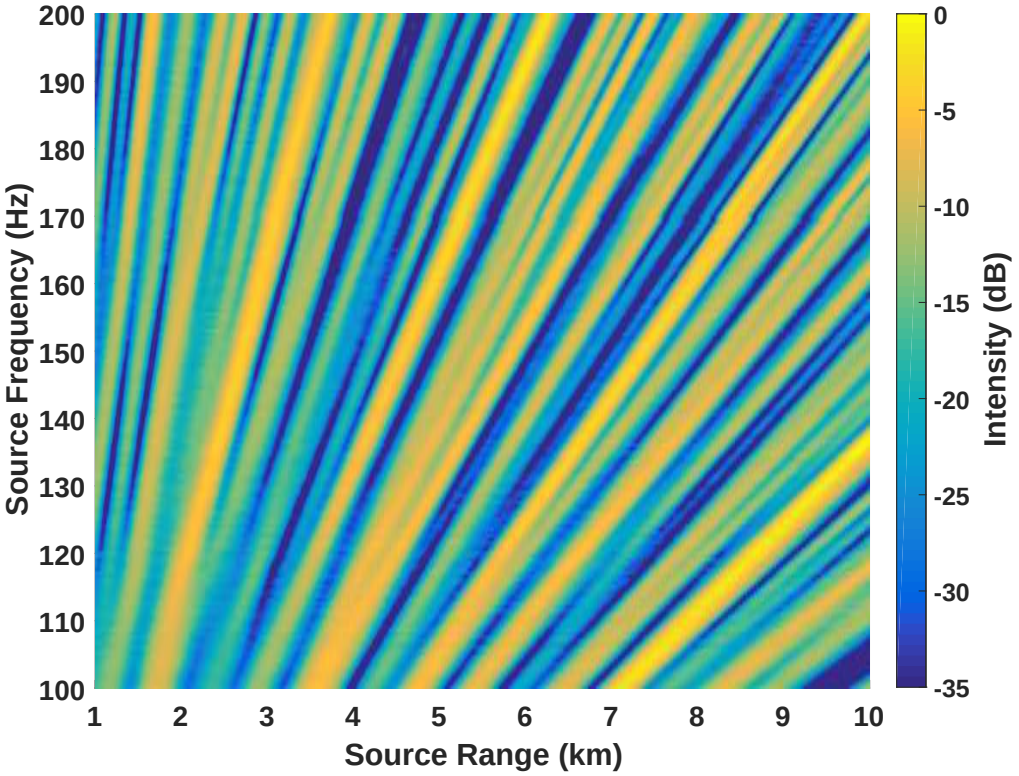

FIGURE 1.1: Received acoustic intensity from a broadband source as a function of frequency and range in a simulated Pekeris waveguide. The striations, or lines of constant intensity, are defined by Equation (1.4) and satisfy Equation (1.9) with $\beta \approx 1$.

broadband, band-limited white noise signal as a function of source-receiver range, or $I(r, \omega)$.

Traditionally, waveguide invariance has been analyzed in terms of the patterns that emerge in intensity plots derived from the spectrograms of acoustic data obtained from observing transiting sources with continuous spectral levels [2]. The interference patterns from the superposition of direct-path and multi-path waves (ray theory) or of propagating modes (normal mode theory) within the waveguide form lines of constant intensity in range and frequency, which are commonly referred to as "striation patterns". The general character of this interference structure is governed by the relationship between group and phase velocities of propagating modes

within the medium[1], and the spacings between striations in the $I(r, \omega)$ surface can be computed using the value of β that characterizes the environment [2]. To better explain this relationship, the parameter β is now introduced and defined as the negative ratio of the change in phase slowness to that of group slowness between an adjacent pair of propagating modes [3]:

$$\beta \equiv \frac{-dS_p^{mn}}{dS_g^{mn}} = \frac{-(S_p^n - S_p^m)}{S_g^n - S_g^m} \tag{1.1}$$

This can be rewritten to show a linear relationship with β^{-1} as:

$$S_g^n = S_g^m - \frac{1}{\beta} dS_p \tag{1.2}$$

Here, S_g^n is the group slowness (inverse group velocity) and S_p^n is phase slowness (inverse phase velocity) for the n^{th} mode, which is adjacent to the m^{th} mode. The linear relationship between group and phase slowness across an entire group of propagating modes, which is implied by a constant β, can be expressed as follows [3]:

$$S_g^n = S_g - \frac{1}{\beta}(S_p^n - S_p) \tag{1.3}$$

where S_g and S_n refer to average phase and group slowness for a group of modes. Equation 1.3 can be viewed as a requirement that must (approximately) hold for β to be considered stable within a particular acoustic environment; that is, a linear relationship must exist between group and phase slowness.

In the ideal isovelocity Pekeris model, β is approximately constant across all propagating modes[4]. However, in real-world, shallow water waveguides, β is approximately constant when reflection-based propagation dominates the modal sum [3], which means that non-constant, highly-variable β is possible, particularly in deep water or areas with rapidly-changing bathymetry or sound speed profiles [2]. This leads to an understanding that, for practical purposes, β will be both mode-

and frequency-dependent, and estimates are considered to be centered about some average frequency and mode number [3].

In terms of range r and frequency ω, β is defined through lines of constant intensity I determined by

$$\frac{\partial I}{\partial \omega}\delta\omega + \frac{\partial I}{\partial r}\delta r = 0 \tag{1.4}$$

To see the relation to β, the normal mode model of the acoustic pressure field is briefly presented [1]:

$$p(r,\omega) = \sum_m A_m e^{i\xi_m r} \tag{1.5}$$

where A_m and ξ_m are the amplitude and eigenvalue of the m^{th} mode. The eigenvalue $\xi_m = k_{rm}$ is the radial wavenumber of the m^{th} mode and is a function of angular frequency ω. For simplicity, the depth dependency of the pressure field due to the mode shape function $\Psi_m(z)$ at the source and receiver depth has been omitted, in addition to the spreading loss terms. Acoustic intensity, normalized by impedance $\rho_0 c$, can be written as

$$\frac{I(r,\omega)}{\rho_0 c} = pp^* = \sum_{m,n} A_m A_n e^{i\Delta k_{mn} r} \tag{1.6}$$

where $\Delta k_{mn} = \xi_n - \xi_m$ is the difference in wavenumber between the m^{th} and n^{th} modes, which can also be written as:

$$\Delta k_{mn} = \frac{\omega}{v_n} - \frac{\omega}{v_m} = \omega(S_p^n - S_p^m) = \omega dS_p \tag{1.7}$$

where v_m and v_n are the phase velocities of the m^{th} and n^{th} modes. The slope, $d\omega/dr$, along the isolines in the $I(r,\omega)$ surface given by Equation 1.4 has been shown to be:

$$\frac{d\omega}{dr} = -\frac{\frac{\partial I}{\partial r}}{\frac{\partial I}{\partial \omega}} = -\frac{\omega}{r}\frac{dS_p}{dS_g} = \frac{\omega}{r}\beta \tag{1.8}$$

For a complete derivation of this result, the reader is referred to an ocean acoustics textbook such as [3]. Along these isoline striations in the $I(r, \omega)$ surface, the following relation holds between β, frequency, and range [3]:

$$\frac{\omega}{\omega_0} = \left(\frac{r}{r_0}\right)^{\beta} \tag{1.9}$$

After isolating ω in Equation 1.9, differentiating with respect to range and setting $\beta = 1$, the slope is found to be $d\omega/dr = \omega_0/r_0$. That is, when $\beta = 1$, each isoline has constant slope throughout the entire $I(r, \omega)$ surface, which can be verified visually by examining Fig 1.1. Moreover, when $\beta \neq 1$, but is still positive, the striations are curved, with slopes that either strictly increase or decrease with range, corresponding to $\beta > 1$ and $\beta < 1$, respectively. Importantly, by applying Equation 1.9, a striation can be "projected" in frequency and range from any point, (r_0, ω_0), given β.

The striation patterns are noticeable at source-receiver ranges exceeding several water column depths [2], but are obscured by the Lloyd's mirror effect at closer ranges. In shallow water environments, this means the interference structure could potentially be utilized, in conjunction with β, at ranges as close as just a few cargo ship lengths, or as far as tens of kilometers [1].

Since its discovery, the stability of the parameter β has been debated. Rouseff and Spindel [5] noted that β is perhaps best modeled as a distribution, which is often sharply peaked in shallow water environments where surface-interacting modes dominate, and more diffuse in deep water environments where ducted modes have greater expression. Chuprov also noted a great range of β values in deep water environments, but relative stability near $\beta \approx 1$ in shallow water. Ultimately, stability comes down to whether Equation 1.3 holds [3], but in a more practical manner, and as the experimental results will show, β can generally be used effectively in coastal regions with relatively flat bathymetry [6], which is advantageous since anthropogenic

noise from heavy cargo ships often dominates the acoustic pressure field in such environments [7]. The abundance of this shipping noise, coupled with the availability of real-time GPS location information that is broadcast by all cargo ships through the Automatic Identification System (AIS)[8], depicted in Figure 1.2, provides an excellent opportunity to passively estimate β in such regions using a single, stationary hydrophone. Essentially, the data from a single phone can be processed to produce the spectral content of Figure 1.1, while the GPS data can be used to produce the range axis of the plot, thereby obtaining the interference structure required for estimating the waveguide invariant. One important application of this, which will be explained later in greater detail, is that once a relatively constant β has been estimated for a particular coastal area, the computed interference structure obtained from a different, non-broadcasting ship can later be used to estimate its range to the same receiver.

1.2 AIS data

The Automatic Identification System (AIS), depicted in Figure 1.2 is a suite of equipment, located at well-defined positions on various commercial ships, that continuously broadcasts a variety of information about a vessel such as its speed, heading, and GPS location at intervals from 2 to 10 seconds [8]. Since 2002, AIS has been an international requirement for large sea-going vessels and all passenger ships, as part of an effort to reduce maritime collisions [8]. In the United States, AIS has also been required to be in use on all commercial vessels transiting inland waterways and ports, regardless of the vessel's size, since 2005, as part of increased port security measures [9, 10]. Worldwide, it was estimated in 2009 that more than 40,000 ships carry AIS equipment [9].

Real-time AIS data can be retrieved by querying the United States Coast Guard database, given that stringent security permissions have been granted to the re-

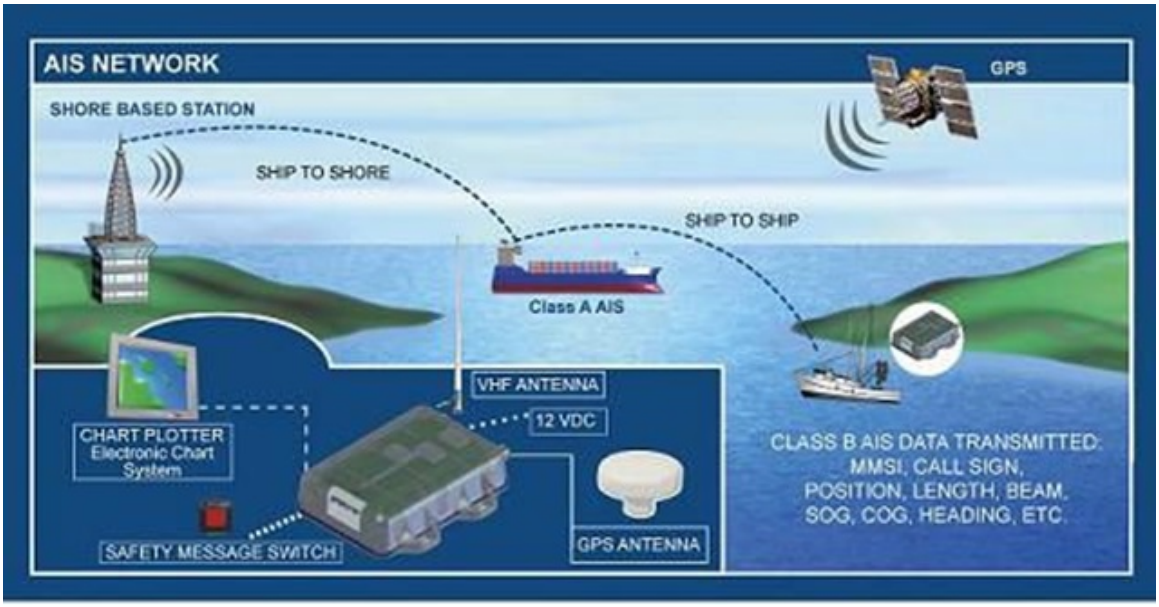

FIGURE 1.2: Representation of AIS in use at sea. Shore based station is part of the National AIS, and ship-to-ship communication is part of the standard AIS. [Image Credit: www.life-raft.com].

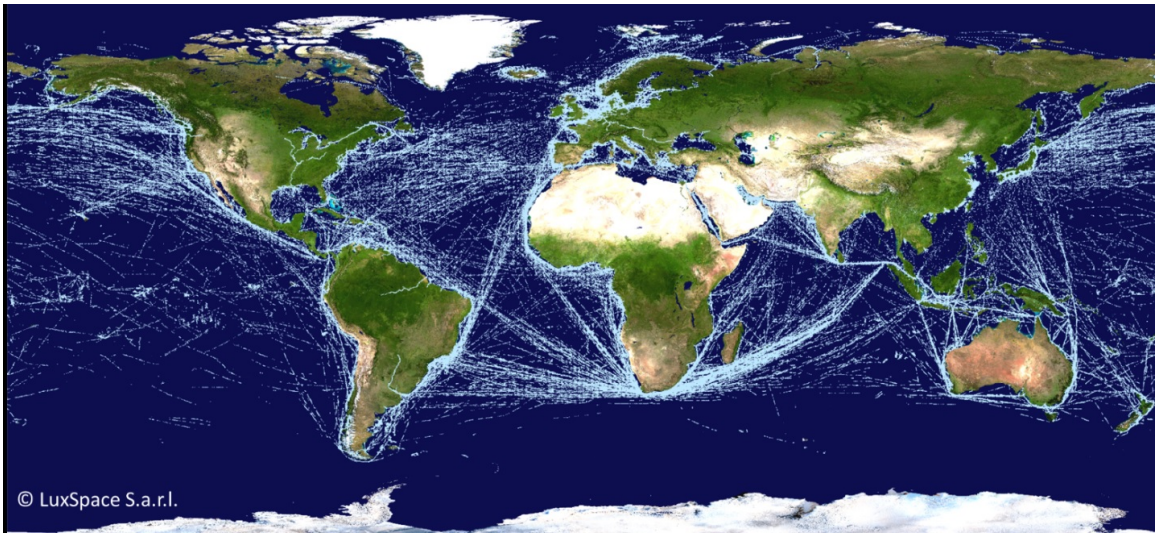

FIGURE 1.3: World map with overlay showing AIS tracks of commercial ships over a 24-hour period [Image Credit: www.esa.int].

questor, and AIS data that has been delayed by more than 96 hours is available to anyone via submission of appropriate Freedom of Information Act (FOIA) forms [10]. However, regardless of the feasibility of university researchers actually obtaining real-time AIS data, the theoretical availability of AIS data has opened the door for ocean acoustic research to view cargo ships as tonal sources with known positions in real time. As Figure 1.3 shows, AIS data is concentrated along coastlines and throughout major trans-ocean shipping lanes. The widespread availability of AIS data has been leveraged in just the past year by Harms, Odom and Krolik [4] as well as Verlinden et al [11], as they have developed methods that use AIS-equipped ships as known sources which can be used to estimate the range of other sources by leveraging the waveguide invariant.

1.3 Comparison to matched field processing

Matched Field Processing (MFP) is a source-localization technique that is conceptually similar to the one proposed in this thesis. MFP techniques are commonly employed in conjunction with a vertical line array (VLA) hydrophone configuration [12], but have also been used with a single hydrophone as well [13]. MFP techniques typically require very precise knowledge of an ocean environment, as they are effectively inverse methods that leverage replica signals derived from spatial point source responses of the medium, computed over an unknown parameter space [12]. They can be highly sensitive to mismatch errors due to sensor noise, uncertainty in sound speed profiles, bathymetry and bottom composition, etc.

In contrast, the waveguide invariant-based technique proposed in this thesis does not require precise environmental knowledge, because it is not an inverse method requiring solutions to the wave equation. Rather than "matching" measured signals to replica signals that are parameterized by a multitude of source and environmental variables, this technique matches intensity along striations that are parameterized by

frequency, range, and β, such as those shown in Figure 1.1 that correspond to $\beta = 1$. The underlying assumption is that a single value of β can adequately characterize a channel, and this is seen to be the case for at least the specific shallow water environment present in the Swellex '96 experiment. This simplicity yields benefits not only in terms of computational efficiency and system cost, but also in robustness. As will be seen in the experimental results, this method yields estimated ranges that are only slightly degraded even when the source signal is turned off for short periods of time, and when the source is towed over varying bathymetry. This robustness to a changing source and environment would not typically be expected from conventional MFP techniques, but it is possible with waveguide invariant-based techniques that leverage the structure of shallow water spectrogram fading patterns.

2

Literature Review

2.1 Previous work to estimate β

Many methods have been proposed in recent years for estimating the waveguide invariant parameter β. In 2000, Aaron Thode developed and published a method using the Radon transform to estimate β, effectively treating the $I(r, \omega)$ surface as an image and seeking to determine the slopes of the striations [6]. A few years later, Rouseff and Yang successfully used a 2-Dimensional discrete Fourier Transform method to estimate β [5, 14], where the 2D-DFT is applied to an $I(r, \omega)$ surface, such as the plot shown in the bottom of Figure 1.1. In 2009, Turgut demonstrated using the Hough transform to estimate Beta in a similar manner, using the slope of striations in the $I(r, \omega)$ surface [15].

However, one shortcoming of these methods is their reliance on obtaining a finely-sampled grid of $I(r, \omega)$ measurements, where the source is assumed to be known such that the $I(r, \omega)$ surface represents the range-varying frequency response of the channel. Although this has been shown to work well with broadband sources in the ocean, Arveson and Vendittis pointed out in 2000 that modern, high-tonnage cargo shipping vessels have a radiated noise spectrum that is dominated by narrowband

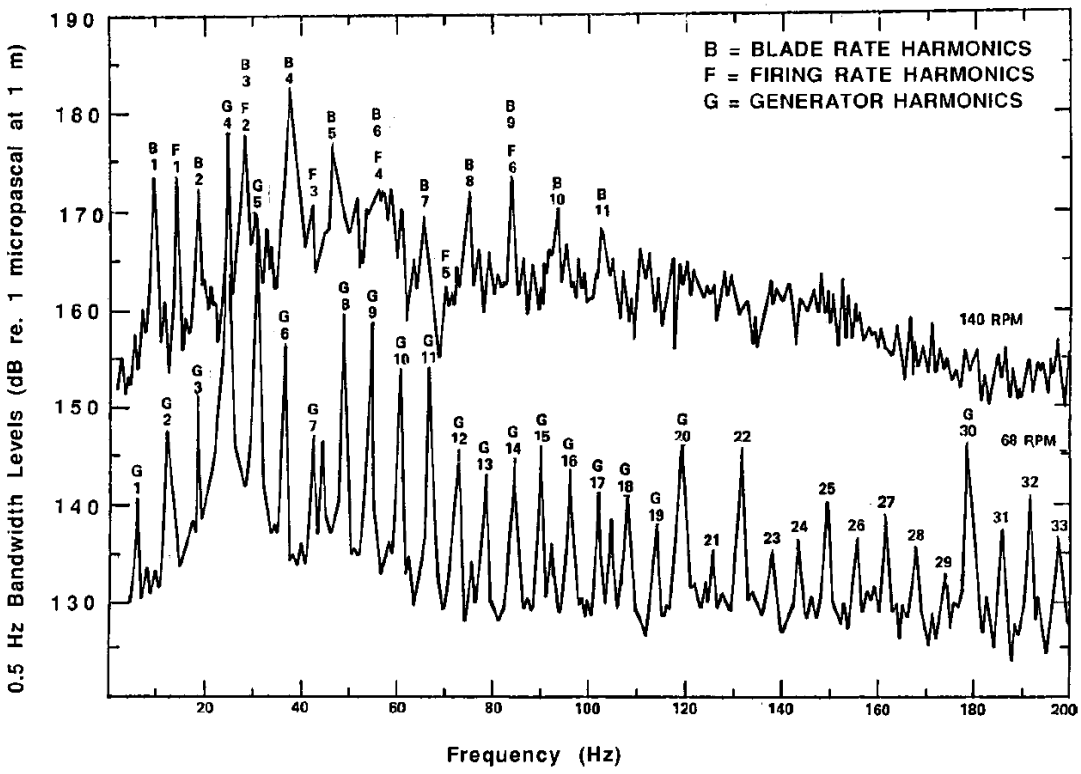

FIGURE 2.1: Example of high-speed (top) and low-speed (bottom) cargo ship emission spectrum. Note that the spectrum is dominated by closely-spaced, narrowband tonals, especially at lower speeds. [Image Credit: Arvesson and Vendittis [7]].

tones, which are referred to as *tonals* [7]. As Figure 2.1 shows, the tonals are typically spaced a few Hertz apart in frequency and have most energy at lower frequencies. This is substantially different from the white noise spectra that were assumed by previous methods, and it raises an important question: is it more useful to have a waveguide invariant-based range estimator that requires known, broadband controlled sources or one that can leverage tonal sources, such as cargo ships? Based on the progression of research, it appears the answer to this question is that an estimator based on tonal sources is preferred.

Finally, in 2014, a method was developed by Harms, Odom, and Krolik[4] that delivered such an estimator. They derived a hybrid maximum-likelihood estimator

for β under a model in which the source is tonal with known (or estimated) tonal amplitudes and unknown phases, and the received acoustic pressure field is corrupted by complex Gaussian noise. The model thus seems to be a much more practical fit to the real-world ocean acoustic environment. This method was tested by means of a Monte Carlo simulation using a Pekeris waveguide and a tonal source with three equal-amplitude tonals corrupted by varying levels of additive noise and was shown to yield an estimate of $\beta = 0.93$, which is very close to the value of 1.0 that would be expected for a shallow-water environment with isovelocity sound speed profile and constant bathymetry. Note that my work, which will be described in detail in the next chapter, picks up from this point and further validates this method by using higher fidelity Kraken simulations, as well as hydrophone data obtained from the Swellex '96 experiment.

2.2 Previous work using the waveguide invariant to estimate range

Now that we have discussed the recent body of work for estimating the waveguide invariant parameter β, we can move on to covering work involving the application of β to range estimation. One of the applications of the waveguide invariant, and indeed the primary application of the research presented in this thesis, is estimating the range of an acoustic source using a single hydrophone.

2.2.1 Estimating range of broadband sources using β

As mentioned in the previous section, Aaron Thode presented a method for estimating β using Radon transforms, given a broadband white noise source, in 2000 [6]. In that paper, Thode also presented a method to estimate the source range using the estimated value of β, which also involved the Radon transform. Thode demonstrated that his method was able to estimate the range of a source in the Swellex-3 experiment, which was performed off the coast of San Diego in 1993, with a reported

accuracy of about 10% [6]. In that experiment, the source was transmitting a pseudo-random noise sequence with 150 Hz bandwidth and relatively high Signal-to-Noise Ratio (SNR) [6]. Although this method, like many other waveguide invariant-based ranging techniques, requires minimal a priori environmental knowledge, the method does require the environment to have a relatively flat bathymetry [6], in order to yield a stable estimate of β.

In 2007, Tao, Hickman, and Krolik [16] described a method for estimating the range and time of the *closest point of approach* (CPA) of a moving surface ship, as well as the ratio of radial velocity to range at the time of CPA, $\frac{v_r}{r_{CPA}}$, using only the pressure field measurements of a single hydrophone. Their method involved processing the intensity surface of the spectogram of the received pressure signal, where the source is assumed to be broadband, but not necessarily tonal [17]. Their experiment was conducted locally at Jordan Lake and was shown to be robust to interfering sources, as it was able to separately identify the test surface vessel, which was a pontoon boat, from a speedboat which was also operating in the area, and estimate the range and velocity of both sources. Separation was achieved by applying a Hough transform to the received spectrogram, allowing the time-varying received spectrum from each of the two surface ships to be recovered. A key assumption made in their processing is that β is approximately unity, which is a common assumption to make in shallow water environments [18], although their method does allow for estimated values of β to be used instead. Their results showed the ability to estimate r_{CPA} with an accuracy of about 4 percent. Overall, this result demonstrated the waveguide invariant can be useful in ranging real-world sources in shallow water environments using only a single hydrophone, although it should be pointed out that the lake environment is different from a coastal environment, and it is also desirable to obtain source range estimates before the source passes through the CPA.

In 2010, Zhen-dong and Hao-zhong published an article [19] proposing yet an-

other method of estimating the range of a broadband source using only a single hydrophone and the waveguide invariant. Their method was unique in that it attempted to calculate a distinct value of β for each pair of propagating modes, rather than estimating a single value of beta that covers a range of modes. They reasoned that this approach is more appropriate since β is approximately invariant to frequency and range for a given pair of modes [19]. To separate the modes, the authors used the MUSIC (MUltiple SIgnal Classification) algorithm. Their method relies on having a broadband "guide source" at a known range, which they can use to estimate the range to other broadband sources. They conducted two experiments in the Yellow Sea and Laoshan Bay using underwater explosions at known locations as their guide sources [19]. They were able to estimate the range to several explosions with accuracies of 5 to 10 percent, at ranges up to 20km. However, they note that one downside to their method is that they expect the accuracy of the range estimation to be degraded when the guide source or unknown sources do not have flat spectra [19]. Overall, this result confirmed the applicability of the waveguide invariant to distant source estimation, but it did not address the need for estimating the range to tonal sources, such as cargo ships.

2.2.2 Estimating range of tonal sources using β

In 2009, Kevin Cockrell and Henrik Schmidt published an article [20] in which they described a "robust" method of performing passive range estimation of an underwater acoustic source by leveraging the waveguide invariant. Their method utilized a 2D-DFT on the received spectrogram and also applied a low-pass filter based on maximum and minimum group velocities for expected propagating modes to obtain a global estimate of β. To test their method, they deployed an autonomous underwater vehicle equipped with a hydrophone to proceed on a course at a fixed radial velocity toward a stationary source transmitting a pseudo-random noise sequence.

Under this scenario, their method was able to estimate the range of the source with an accuracy of 25 percent. Overall, this result presented an alternative to Thode's Radon transform-based method [6] for estimating β and the range of a white noise source.

In 2012, Rakatonarivo and Kuperman published a paper [18] in which they stated that estimating the range to a source requires one of two things: 1) an array of hydrophones of sufficient horizontal extent for beamforming techniques to be applied, or 2) an estimate of β and an estimate of the source's radial velocity. They took the latter route and introduced a novel method for estimating source radial velocity by means of a "field differencing method," which uses a discrete Fourier Transform of the cross-correlation of the received pressure field. Using this method, they were able to estimate the range of a tonal source in the Swellex '96 experiment with approximately 20 percent accuracy. Note that this result is perhaps the most significant related work to this thesis research, as the results that will be shown in Chapter 4 are drawn from the same experiment. This result is significant, as it demonstrates the ability to leverage the waveguide invariant for estimating the range to tonal source in an environment with varying bathymetry.

Most recently, Chris Verlinden, a collaborator on the MURI grant which is funding this research, published a paper [11] in 2015 in which he described a method for localizing sources by using a cross-correlation library, which is populated using pairs of hydrophones spatially separated by several hundred meters. The waveguide invariant is leveraged to interpolate and create replica vectors corresponding to positions that fill a search space. Verlinden's method for populating the library leverages the availability of AIS data, which is required by law to be in use on all but the smallest classes of sea-faring vessels [11], and locates unknown sources by searching for peaks in the cross-correlation of the received acoustic signals and the cross correlation library replica vectors. Verlinden's method was shown to work well

on real-world tonal sources (cargo ships), but does not explicitly require the sources to be tonal. This method was shown to be quite robust, as the library that was constructed on the first day of the Noise '09 experiment was used to localize transiting cargo ships 5 days later [11].

2.3 Summary

This field of research began in the early 1980's with the discovery of the waveguide invariant [1] and began to be formally applied to the problem of estimating underwater acoustic source range in the early 2000's [2, 5, 6]. Many different methods have been proposed by which the value of the waveguide invariant parameter, β, can be estimated [4, 6, 18, 20, 21]. The first methods required knowledge of the range of a controlled broadband source, while recent methods have begun looking at tonal sources, especially since the widespread adoption of AIS on commercial vessels in the mid-late 2000's [8]. Similarly, many different methods have been proposed by which the waveguide invariant can be used to estimate source range using a single hydrophone [4, 6, 16, 18, 20]. As with waveguide invariant estimation, the first methods that were proposed for ranging required unknown sources to be broadband [6, 15, 16], while more recent methods have focused on estimating the range of tonal sources using the waveguide invariant [4, 11]. As AIS data became more widely available, the focus on tonal sources became even more relevant, as the high volume of cargo shipping traffic means that known, tonal sources now abound along the coastlines of the United States and other world economic powers. This thesis research builds on these recent developments by using knowledge of the range of tonal sources (i.e. commercial shipping vessels equipped with AIS) to estimate β, and then using β to estimate the range of other tonal sources transiting through the same areas of the ocean.

3

Waveguide Invariant-Based Range Estimation

3.1 Estimating β and range to tonal sources

The estimators presented in this thesis build upon the earlier work of Harms, Odom, and Krolik [4], in which they derived a maximum likelihood estimator for striation intensity, given a tonal source. They also derived a maximum likelihood minimum mean-squared error (ML-MMSE) estimator for β that leverages the maximum likelihood estimate of striation intensity. This thesis provides a validation of their β estimator, as well as presents a complementary range-estimation method that is supported by experimental results. Both estimators are now introduced, beginning with the source model which is shared in common.

3.1.1 Modeling received signal

The source is modeled as a sum of pure tones, which is an approximation to a typical commercial cargo shipping vessel, which has an acoustic emissions spectrum that is dominated by fundamental and harmonic tonals from onboard diesel generators, propulsion engines, and propeller cavitation [7]. The source signal, $s(t)$, is written

as follows:

$$s(t) = \sum_{\omega \epsilon \Omega} a(\omega) e^{j(\omega t + \phi(\omega))} \tag{3.1}$$

Here, ω, is the center frequency of each narrowband tonal in the source spectrum. The amplitude of a particular tonal, $a(\omega)$, is assumed to be either known a priori or well-estimated. For the processing required by this estimator, amplitudes $a(\omega)$ can be relative, rather than absolute, measurements. That is, the estimator only needs an estimate of the amplitude of each tonal component relative to the highest amplitude tonal being processed. The phase of each tonal, ϕ, is assumed to be unknown and uniformly distributed, but constant over an observation interval of a few seconds:

$$\phi(\omega) \sim \mathcal{U}(-\pi, \pi) \tag{3.2}$$

The received signal is a hydrophone measurement, $p_n(r,t)$, and is modeled as a sum of the time-varying acoustic pressure due to the source at range r, with additive noise:

$$p_n(r,t) = p(r,t) + n(r,t) \tag{3.3}$$

Let $p_n(r,\omega)$ be the complex amplitude of the sampled noisy hydrophone measurement transformed to the frequency domain, where ω is again the center frequency of a given source tonal. In practice, $p_n(r,\omega)$ can be obtained through a Discrete Fourier Transform (DFT) of a sampled form of $p_n(r,t)$. After normalizing for signal length, this measurement is a sum of noisy and noise-free components as follows:

$$p_n(r,\omega) = p(r,\omega) + n(r,\omega) \tag{3.4}$$

The additive noise component $n(r,\omega)$ is modeled as a circularly-symmetric complex normal random variable with variance σ_n^2:

$$n(r,\omega) \sim \mathcal{CN}(0, \sigma_n^2) \tag{3.5}$$

However, the noise variance, σ_n^2, cannot be measured directly and must instead be derived from other quantities, such as the norm of $n(r, \omega)$. This quantity is Rayleigh distributed, with scale parameter equal to the standard deviation of the noise component:

$$\|n(r, \omega)\| \sim Rayleigh(\sigma_n) \tag{3.6}$$

The expected value of $\|n(r, \omega)\|$ is as follows:

$$E\left[\|n(r, \omega)\|\right] = \frac{1}{2}\sigma_n\sqrt{2\pi} \tag{3.7}$$

Thus, the noise variance, σ_n^2, can be estimated directly from the sample mean, $\bar{n}$, of spectral measurements taken at a series of N ranges, $\vec{r}$, spanning the horizontal axis of the $I(r, \omega)$ surface and F frequencies $\omega_i + \delta\omega, i = 1...F$ that are slightly offset from the tonal frequencies of interest:

$$\bar{n} = \frac{1}{FN}\sum_{i=1}^{F}\sum_{j=1}^{N}\|n(r_1^{(j)}, \omega_i + \delta\omega)\| \tag{3.8}$$

where $r_1^{(j)}$ is the j^{th} component of the length-N vector $\vec{r}$. The offset, $\delta\omega$, is intended to reduce the contribution of the signal to the noise measurement, and care should be taken to choose an appropriate windowing function to facilitate this.

Another approach could involve computing the sample mean from a smaller series of measurements taken only in the vicinity of individual striations, in which case $\vec{r}$ would be constructed using Equation 1.9. That is, rather than spanning the horizontal axis of the $I(r, \omega)$ surface, $\vec{r}$ would instead consist of discrete ranges corresponding to a particular projected striation. In that case, the sample mean, $\bar{n}$ would then be a vector of length N, which is equal to the number of projected striations:

$$\bar{n}_j = \frac{1}{F}\sum_{i=1}^{F}\|n(r_i^{(j)}), \omega_i + \delta\omega)\| \tag{3.9}$$

where $r_i^{(j)}$ is the range corresponding to the i^{th} tonal frequency component of the j^{th} projected striation across the $I(r, \omega)$ surface, and is computed in accordance with Equation 1.9 as follows:

$$r_i^{(j)} = r_1^{(j)} \left(\frac{\omega_i}{\omega_1} \right)^{1/\beta} \tag{3.10}$$

Once the desired measure of sample mean is computed, the estimated noise variance is found by:

$$\hat{\sigma}_n^2 = \frac{2\bar{n}^2}{\pi} \tag{3.11}$$

In the case of the per-striation noise estimation method, $\hat{\sigma}_n^2$ would be a vector of length N, with each individual component being found through application of Equation 3.11. Once the noise variance is estimated, the noise-free acoustic intensity at the hydrophone can be obtained through the method described in the following section.

3.1.2 Modeling measured intensity

Time-average acoustic intensity, denoted by $\langle I(t) \rangle$, can be expressed as one half the square of the complex pressure magnitude divided by acoustic impedance [3]:

$$\langle I(t) \rangle = \frac{\|p\|^2}{2\rho_0 c} \tag{3.12}$$

Assuming acoustic impedance is roughly constant across the tonal frequencies of interest, a new term I_n is introduced, which is a measure of intensity that is scaled by acoustic impedance. This is desirable, as it can be obtained directly from noisy hydrophone pressure measurements:

$$I_n = 2\rho_0 c \langle I_n(t) \rangle = \|p + n\|^2 \tag{3.13}$$

Using Equation 3.13, the noise-free pressure can be written as the square root of the intensity measurement that would be obtained directly from hydrophone measure-

ments in the absence of noise:

$$p(r,\omega) = \sqrt{I(r,\omega)} \tag{3.14}$$

Next, the noise is separated into in-phase and out-of-phase components, $n_{\parallel}$ and $n_{\perp}$, with respect to the phase of the noise-free pressure:

$$\begin{aligned} I_n(r,\omega) &= \|\sqrt{I(r,\omega)} + n_{\parallel}(r,\omega) + n_{\perp}(r,\omega)\|^2 \\ &= \sigma_n^2 \left(\frac{\sqrt{I(r,\omega)} + n_{\parallel}(r,\omega)}{\sigma_n} \right)^2 + \left(\frac{n_{\perp}(r,\omega)}{\sigma_n} \right)^2 \end{aligned} \tag{3.15}$$

Let the random variable Y be a scaled measurement of the noisy intensity obtained from a hydrophone:

$$Y = \frac{I_n(r,\omega)}{\sigma_n^2} \tag{3.16}$$

From Equation 3.5, since $n(r,\omega)$ is circularly-symmetric complex Gaussian noise, both orthogonal components $n_{\perp}$ and $n_{\parallel}$ are zero mean with variance σ_n^2. It follows that Y is non-central chi-squared distributed, with $k = 2$ degrees of freedom and non-centrality parameter, λ, given by:

$$\lambda = \left(\frac{\sqrt{I(r,\omega)}}{\sigma_n} \right)^2 = \frac{I(r,\omega)}{\sigma_n^2} \tag{3.17}$$

The probability density function of Y is as follows [22, Section 26.4.25]:

$$\begin{aligned} f_Y(y;k,\lambda) &= \frac{1}{2} e^{-(y+\lambda)/2} \left(\frac{y}{\lambda} \right)^{k/4-1/2} I_{k/2-1}(\sqrt{\lambda y}) \\ &= \frac{I_0\left(\sigma_n^{-1} \sqrt{y I(r,\omega)} \right)}{2\sqrt{exp(y + \sigma_n^{-2} I(r,\omega))}} \end{aligned} \tag{3.18}$$

where $I_0(\dots)$ is a modified Bessel function of the first kind.

3.1.3 Estimating noise-free received intensity

The maximum likelihood estimate (MLE) of the noise-free intensity along a striation in the $I(r, \omega)$ surface of a received signal can be obtained by leveraging the physics of the waveguide invariant. Given β and an estimate of the noise-free intensity at some reference range and frequency, (r_0, ω_0), the noise-free intensity of all other points lying on the same striation can be found in accordance with Equation 1.9:

$$I(r_i(n), \omega_i) = I\left(r_0(n)\left(\frac{\omega_i}{\omega_0}\right)^{1/\beta}, \omega_0\right) \tag{3.19}$$

If the value of β in Equation 3.19 is correct (in the sense of adequately describing the fading pattern of the channel), and if the noise variance σ_n^2 is constant and known over the frequency range of tonals Ω, then the scaled noisy measurements of intensity along a striation are independent and identically distributed (i.i.d.) [4], with the density function given by Equation 3.18. The likelihood of a particular value of the noiseless intensity along the n^{th} projected striation, $I(n)$, given scaled measurements $\vec{y}(n)$ of the noisy intensity at each of F tonal frequencies along the striation, which is governed by β, is as follows:

$$\ell(I(n;\beta)|\vec{y}(n)) = \prod_{i=1}^{F} f_Y(y_i(n); I(n;\beta), \sigma_n^2) \tag{3.20}$$

The estimated, maximum likelihood noise-free intensity along a striation is given by:

$$\hat{I}_{ML}(n;\beta) = \underset{I(n;\beta)}{\arg\max}\, \ell(I(n;\beta)|\vec{y}(n)) \tag{3.21}$$

3.1.4 Overview of β estimators

Given an $I(r, \omega)$ surface with sufficient extent in range to project N striations across F desired tonal frequencies Ω, β can be estimated using a variety of methods. These methods, which will be described in further detail in the following sections, each

begin by hypothesizing a vector of β values. For each hypothesized β, striations are projected across the $I(r, \omega)$ surface in accordance with Equation 1.9, and the maximum likelihood estimate of noise-free intensity along each striation is computed in accordance with Equation 3.21. From there, each method proceeds on its own course.

3.1.5 MMSE β estimator

The first method picks up where Section 3.1.4 left off by computing the resulting mean squared error (MSE) between the measured noisy intensities and the ML noise-free intensity estimate along each striation, for each hypothesized β, as follows:

$$MSE(\beta) = \frac{1}{FN} \sum_{i=1}^{F} \sum_{n=1}^{N} \left(\hat{I}_{ML}(n; \beta) - y_i(n) \right)^2 \tag{3.22}$$

β is obtained by minimizing this error:

$$\hat{\beta} = \arg\min_{\beta} MSE(\beta) \tag{3.23}$$

This is presented as the MMSE estimate of β [4]; it is the value of β which minimizes the MSE between the observed intensity I_n and the MLE intensity $\hat{I}_{ML}$ over all projected striations. This estimator is preferred due to its robustness in both real and simulated environments, as demonstrated in Chapter 4.

3.1.6 Maximum likelihood β estimator

Another candidate estimator is one which considers not only the scaled noisy intensity measurements, $\vec{y}(n)$, along each of the N projected striations to be independent, but also treats each striation as an independent data segment. The resulting likelihood of a particular value of β, given all of the scaled noisy intensity measurements across N striations, is then the product of the likelihoods given by Equation 3.20 for each

striation, which is expressed as follows:

$$\ell(\beta|\hat{I}_{ML}(\vec{n},\beta)) = \prod_{n=1}^{N} \ell(\hat{I}_{ML}(n;\beta)) \tag{3.24}$$

β is then estimated to be the value which maximizes the likelihood given by Equation 3.24:

$$\hat{\beta} = \arg\max_{\beta} \ell(\beta|\hat{I}_{ML}(\vec{n},\beta)) \tag{3.25}$$

3.1.7 Maximum a posteriori β estimator

The next two estimators employ prior knowledge regarding the distribution of the waveguide invariant to obtain a posterior distribution of β. Let x represent the observations (scaled noisy acoustic intensity measurements). Using Bayes' rule, the posterior distribution of the waveguide invariant, conditional to the observations, $p(\beta|x)$, is proportional to the product of the likelihood and the prior density as follows:

$$p(\beta|x) \propto p(x|\beta)p(\beta) \tag{3.26}$$

Using the maximum a posteriori (MAP) estimator, β is estimated to be the value which maximizes the posterior density function given in Equation 3.26:

$$\hat{\beta} = \arg\max_{\beta} \; p(\beta|x) \tag{3.27}$$

This method is equivalent to employing a "hit or miss" cost function, in which one incorrect estimate is equally detrimental as another, if they are both further from the true value by more than a specified amount, δ. In reality, however, this is not the case. As will be seen in the experimental results shown in Chapter 4, an incorrect estimate of β that is off by .01 to 0.1 can still be very useful in estimating the range to a tonal source, with larger misses giving less accurate estimates than smaller misses.

Thus, the cost function of this estimator does not align well with experimental results and will not be considered further.

3.1.8 Posterior mean β estimator

The final estimator considered is one which estimates β to be the mean value of the posterior density, $p(\beta|x)$:

$$\hat{\beta} = E[p(\beta|x)] \tag{3.28}$$

where $E[\bullet]$ is the expected value operator. Let $\vec{\beta} = [\beta_1 ... \beta_M]^T$ be a length-M vector of hypothesized β values. The posterior mean is approximated by multiplying each hypothesized β by its normalized density:

$$\hat{\beta} = \frac{1}{c} \sum_{i=1}^{M} [\beta \; p(\beta|x)] \Big|_{\beta=\beta_i} \tag{3.29}$$

where the normalizing constant, c, is computed as follows:

$$c = \sum_{i=1}^{M} p(\beta|x) \Big|_{\beta=\beta_i} \tag{3.30}$$

This method is equivalent to employing a quadratic cost function, and could be useful in scenarios when additional prior information is known, specifically regarding the distribution of β values.

For the remainder of this work, the estimators used in simulation, as well as for range estimation, will be based on the MMSE estimator presented in Section 3.1.5. As will be seen in Section 3.2, this allows for a high degree of consistency between the waveguide invariant and source range estimators, while still allowing each to operate with minimal prior knowledge about the acoustic environment. However, in practice, if additional knowledge regarding the distribution of β is available, it would likely be beneficial to employ that using a method similar to this.

3.1.9 Simulation: MMSE β estimator

Kraken normal mode ocean acoustic simulation software was used to model a shallow water environment with an isovelocity sound speed profile. This environment was chosen because the value of β is known to be very close to unity for this case [3], and Equation 1.3 holds for all propagating modes and frequencies. The channel frequency response magnitude was computed for 20 tonals evenly spaced between 200 Hz and 400 Hz using a 200 meter deep, isovelocity channel with sound speed of 1500 m/s and bottom properties as depicted in Figure 3.4. The value of β for this environment is estimated to be 1.02, as shown in Figure 3.1, indicating excellent agreement with the canonical $\beta \approx 1$ shallow water value. Two other environments were also simulated, which used sound speed profiles and bottom properties as measured during event S5 of the Swellex96 experiment [23]. Both environments involved a receiver at the bottom of the water column, to approximate the positioning of the hydrophones in the HLAS array, and used a 6km long simulated source tow. With a shallow simulated source at 9m depth transmitting 4 tonals evenly spaced between 110 and 170 Hz, β is estimated to be 1.20, and with a deep source at 54m the estimated β increases to 1.24.

These results compare favorably to those obtained using real data from hydrophone #1 in the HLAS array from a 40 minute window of Event S5. Using the real data, β was estimated to be 1.20 when using 4 tonals from the shallow source, which had a reported depth of 9m, at frequencies of [109 127 145 163] Hz. For the deep source, at a reported depth of 54m, β was estimated to be 1.29 when using 4 tonals at frequencies of [112 130 148 166] Hz.

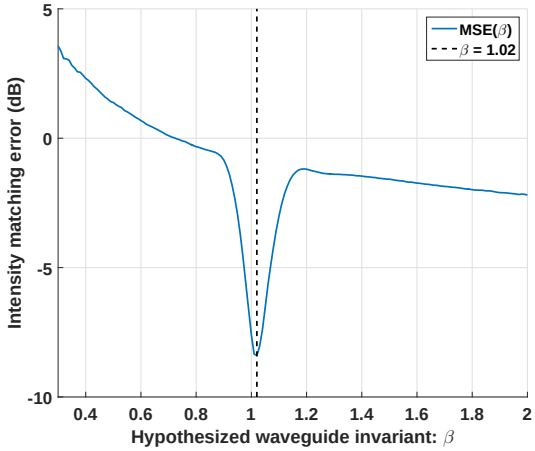

(a) Simulation: isovelocity SSP

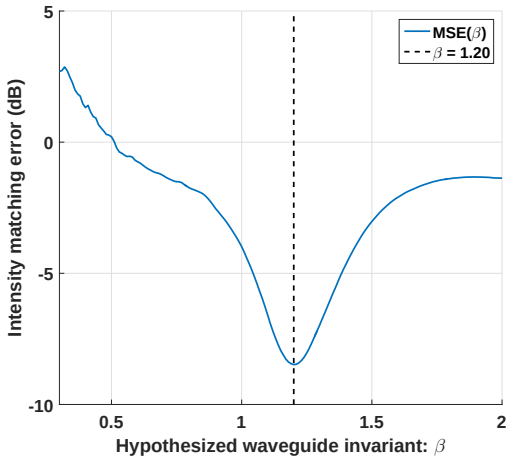

(b) Simulation: SW96 environment w/ shallow source

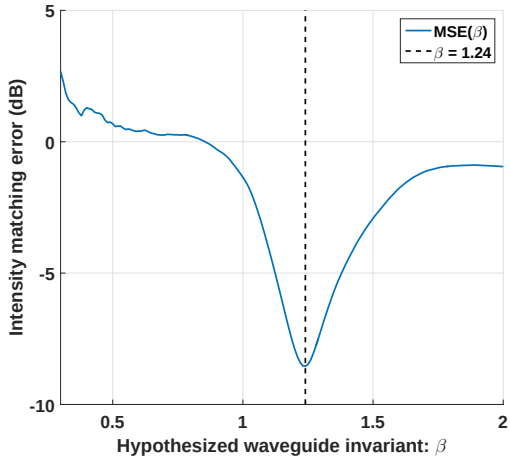

(c) Simulation: SW96 environment w/ deep sourec

FIGURE 3.1: Plots of mean squared intensity matching error vs hypothesized β values for simulated environments with a stationary receiver and moving source transiting a 6km track: (a) isovelocity channel with source and receiver at 9m depth, (b) real SW96 environment with receiver at bottom of water column and shallow source at 9m depth, (c) SW96 environment with receiver at bottom of water column and source at 54m depth. For the real environments of (b) and (c), estimated β is seen to increase slightly when the source depth is increased from 9m to 54m.

3.2 Range estimation using β

Once an estimate of β has been obtained for a channel, the range to a tonal source can be estimated by means of a similar MLE-based method. One important requirement of this method, however, is that a range rate estimate, $\hat{v}_s$, is required in order to compute a vector of hypothesized ranges $\vec{r_0} = r_1^{(1:n)}$ from a single initial range estimate r_0:

$$r_1^{(m+1)} = r_1^{(m)} + \hat{v}_s \Delta t \tag{3.31}$$

For each range hypothesis $\vec{r_0}$, striations corresponding to $\hat{\beta}$ are then computed as follows:

$$r_i^{(n)} = r_1^n \left(\frac{\omega_i}{\omega_1} \right)^{1/\hat{\beta}} \tag{3.32}$$

Now, rather than searching for the value of β which minimizes the striation-matching error, the ML-MMSE estimate $\hat{\beta}$ is used to search for the initial range r_0 which minimizes striation-matching error. That is,

$$MSE(r_0) = \frac{1}{FN} \sum_{i=1}^{F} \sum_{n=1}^{N} \left(\hat{I}_{ML}(n; r_0, \hat{\beta}) - y_i(n) \right)^2 \tag{3.33}$$

The ML-MMSE estimate $\hat{r}_0$ is obtained by minimizing this error:

$$\hat{r}_0 = \arg\min_{r_0} MSE(r_0) \tag{3.34}$$

A block diagram highlighting the similarities and differences between the β and source range estimators is shown in Figure 3.2.

To evaluate the performance of the proposed range estimator through rigorous simulation, Kraken was used to produce an $I(r, \omega)$ surface corresponding to Event S5 of the Swellex96 experiment. The environmental parameters used are shown in Figure 3.4, with the exception that the sound speed profile from Station #4 was used

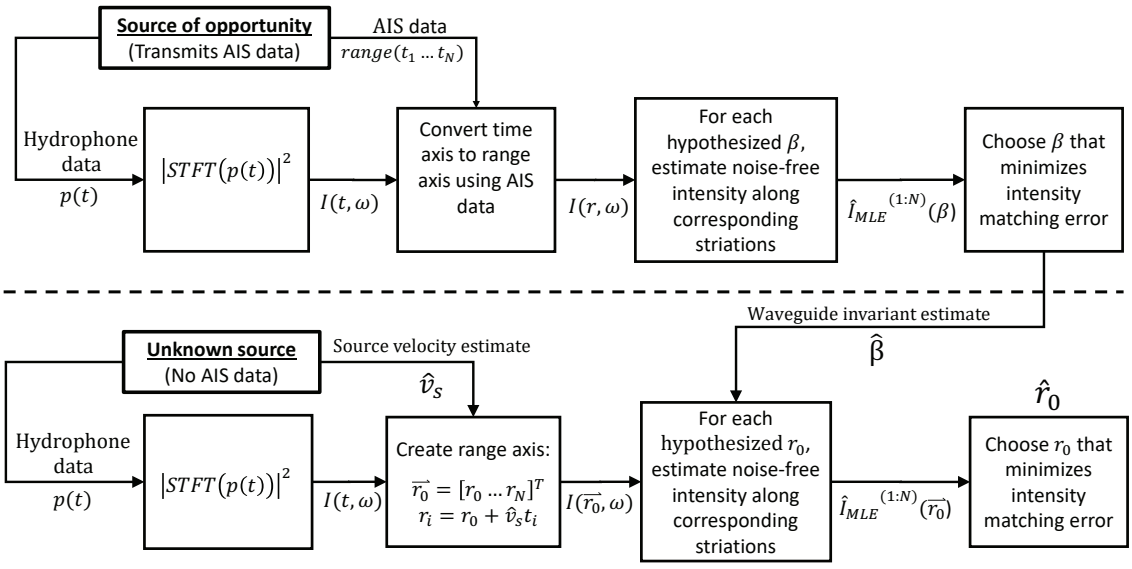

FIGURE 3.2: Block diagram of the processing chain for estimating β and source range. The top half shows the β estimator, while the bottom half depicts the range estimator. Note the extra requirement of a source velocity (range rate) estimate for the range estimator.

in lieu of the profile shown, due to spatial proximity to the HLAS array and temporal proximity to Event S5. In the simulation, a source at depth 54m transited a 4km track, moving radially away from the source while transmitting 4 tones evenly spaced between 110 Hz and 170Hz. The source velocity is assumed to be well-estimated, and the results from employing two different estimates of β are presented in Figure 3.3.

The first estimate, $\hat{\beta} = 1.20$ is the value obtained previously for the environment described in Section 3.1.6E, which is identical except that the source was at 9m depth and transited a 6km track. This corresponds to the estimate of β that could be expected from analyzing the real hydrophone data from Event S5, using tonals corresponding to the shallow source. The second estimate, $\hat{\beta} = 1.24$ is the value obtained previously through simulation in which a source at 54m depth transits a 6km track. This corresponds to the estimate of β that could be expected using tonals

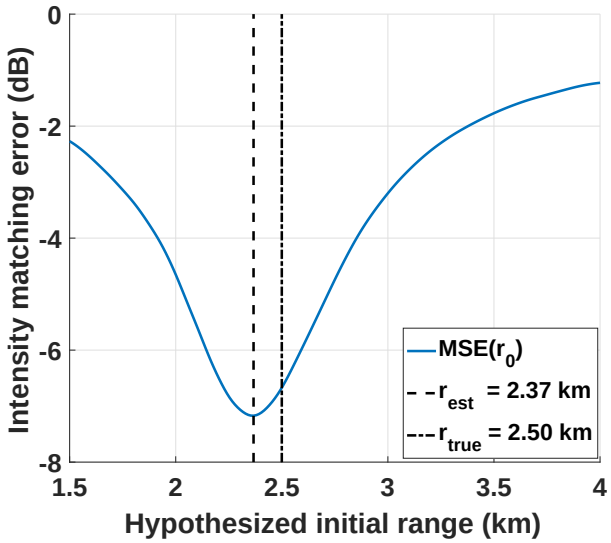

(a) Simulation: mismatched depth localization

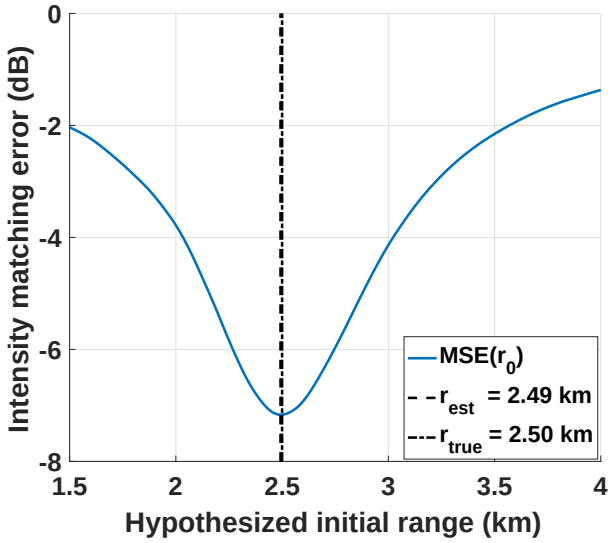

(b) Simulation: matched depth localization

FIGURE 3.3: Plots of mean squared intensity matching error vs hypothesized source ranges for simulated environments with a stationary receiver and moving source: (a) SW96 environment with receiver at bottom of water column and deep source at 54m depth, using previously-obtained shallow source estimate $\beta = 1.20$ (c) SW96 environment with receiver at bottom of water column and deep source at 54m depth, using previously-obtained deep source estimate $\beta = 1.24$

corresponding to the deep source in Event S5.

300 Monte Carlo simulations were run using 9dB SNR per tone, which is the estimated SNR for hydrohpone #1 from the HLAS array for both the shallow and deep source signals, and the plots in Figure 3.3 depict the average matching error as a function of hypothesized source range. For the shallow source estimate $\hat{\beta} = 1.20$, the results show a well-defined minimum mean-squared intensity matching error at an estimated initial range of 2.37km, which is 130m less than the true range of 2.5km. In general, for cases of mismatched β values - the estimated range will be less than the true range when the value $\hat{\beta}$ given to the range estimator is less than the true value of β for the channel, and vice versa. Using the deep source estimate $\hat{\beta} = 1.24$, the range was estimated to be 2.49km.

These results indicate that range-independent shallow water environments can be characterized reasonably well by a single value of β. In the first case, an estimate of β obtained from a shallow source transiting a 6km track was used to estimate the range to a deep source along a 4km track with an error of 5%. In the second case, an estimate of β obtained from a deep source was used to estimate the range to another deep source with near perfect accuracy. In the next section, the performance of the estimator is examined using real data from a shallow water experiment with slowly-varying bathymetry.

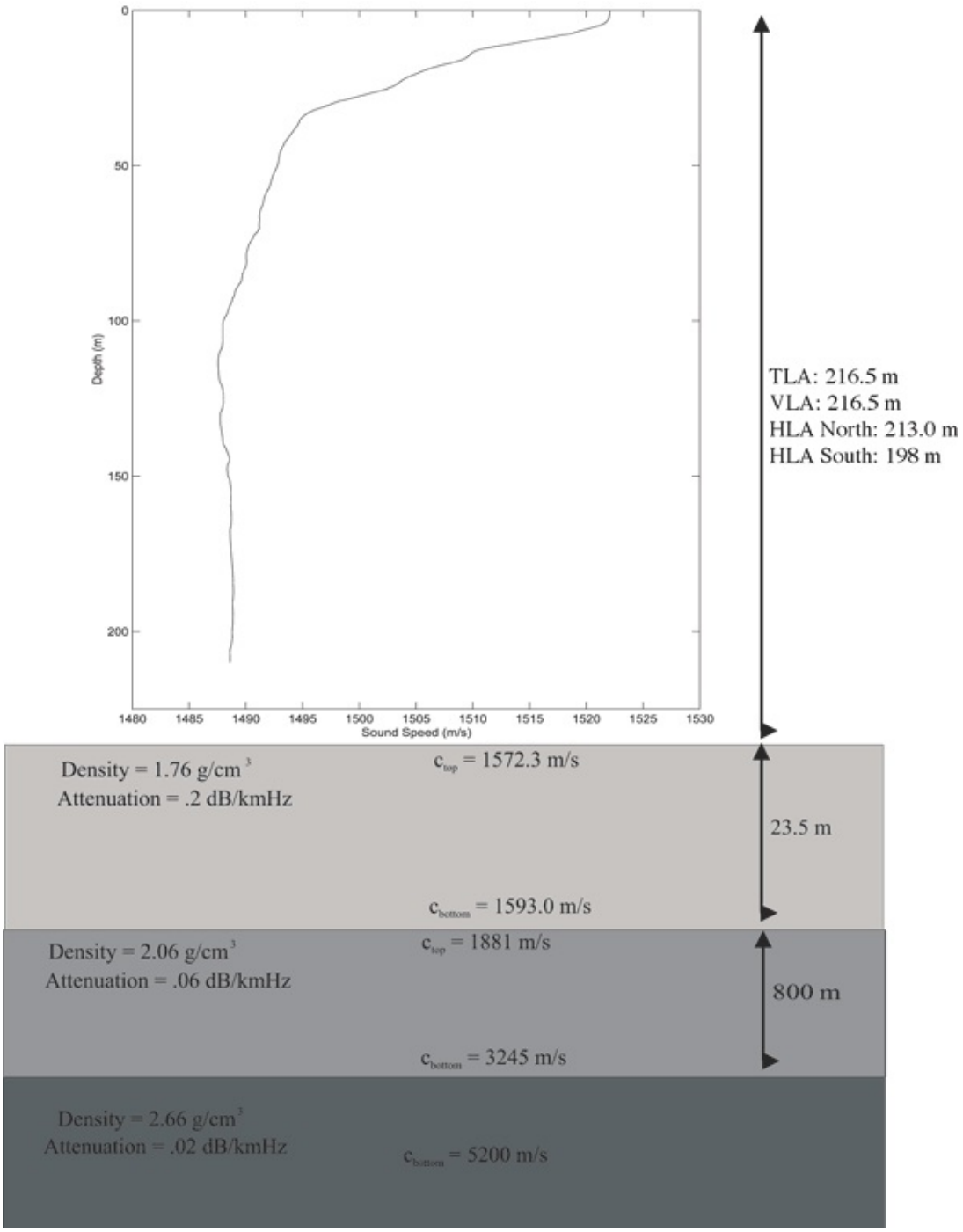

FIGURE 3.4: Graphical depiction of Swellex 96 environmental parameters used for all simulations. Source http://swellex96.ucsd.edu/environment.htm.

4

Experimental Results

4.1 Experimental Results

The Swellex 96 experiment was conducted in May 1996 in the shallow coastal waters near Point Loma, California [23]. Hydrophone data from Event S5, which is a subset of the SW96 experiment and is depicted in Figure 4.1, was selected for two primary reasons: first, two well-defined tonal sources, one shallow and one deep, were employed; second, the event occurred in a shallow-water region with relatively flat bathymetry (< 100 meters change in water column depth throughout the event).

Event S5 was approximately 75 minutes in length. A research vessel equipped with GPS towed two sources along the path indicated by the blue diamonds in Figure 4.1. A deep source was towed at a depth of 54m and emitted 5 separate sets of 9 tonals, with each set having constant amplitude, except for a few periods when the tonal waveforms were turned off and frequency-modulated (FM) chirps were transmitted. The shallow source was towed at a depth of 9m and emitted a single set of 9 tonals with constant amplitude for the duration of the experiment. Based on an analysis of matched field processing results, as well as spectrograms from various

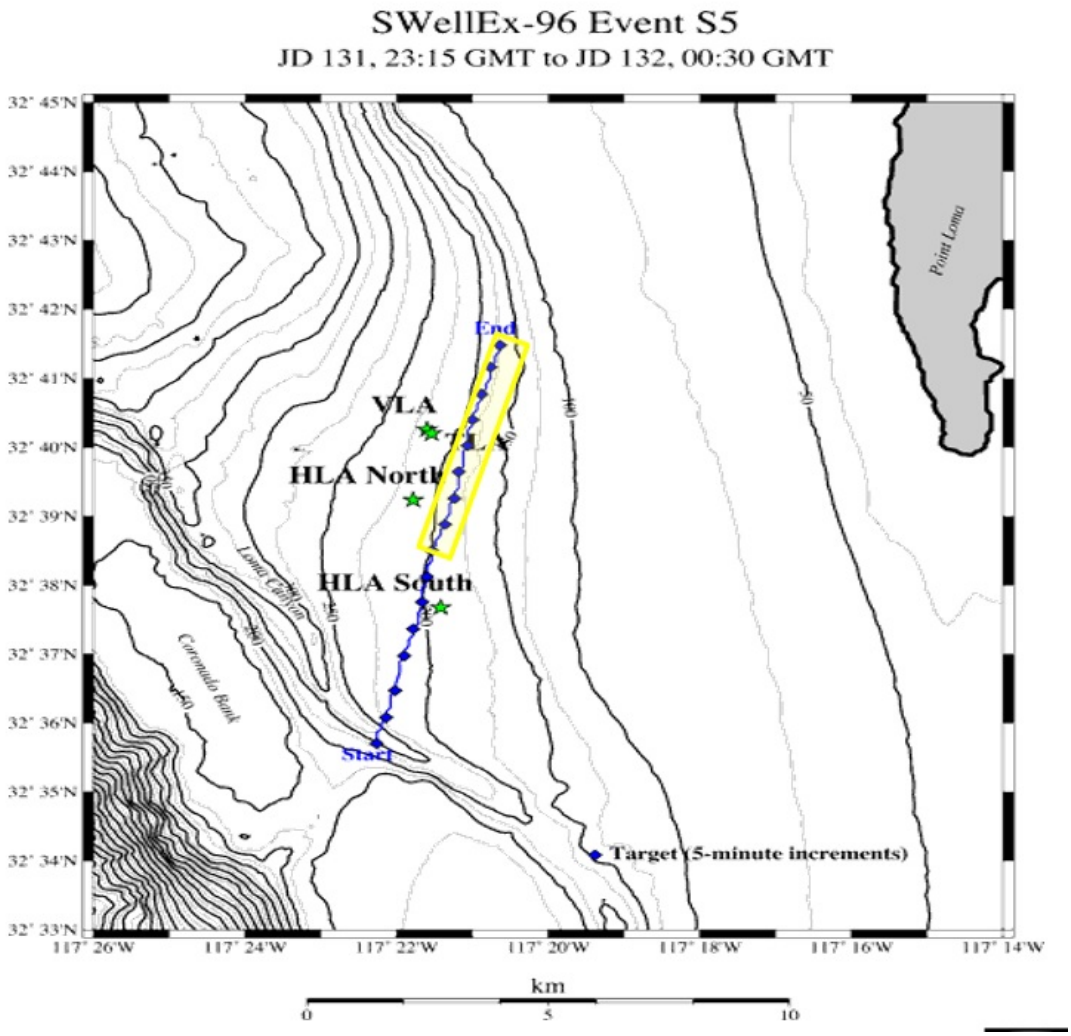

FIGURE 4.1: Overview of Event S5 of Swellex '96 Experiment. Source http://swellex96.ucsd.edu/s5.htm.

hydrophones from each array, the position of the deep source was estimated to lag that of the tow ship by approximately 39 seconds, and the shallow source lagged the tow ship by approximately 13 seconds. Using these estimates, the positions of the shallow and deep sources were computed by delaying the GPS data from the tow ship accordingly.

Four fixed arrays of 16 hydrophones each recorded the event. Data from the Horizontal Line Array South Hydrophone #1 covering the last 40 minutes of this

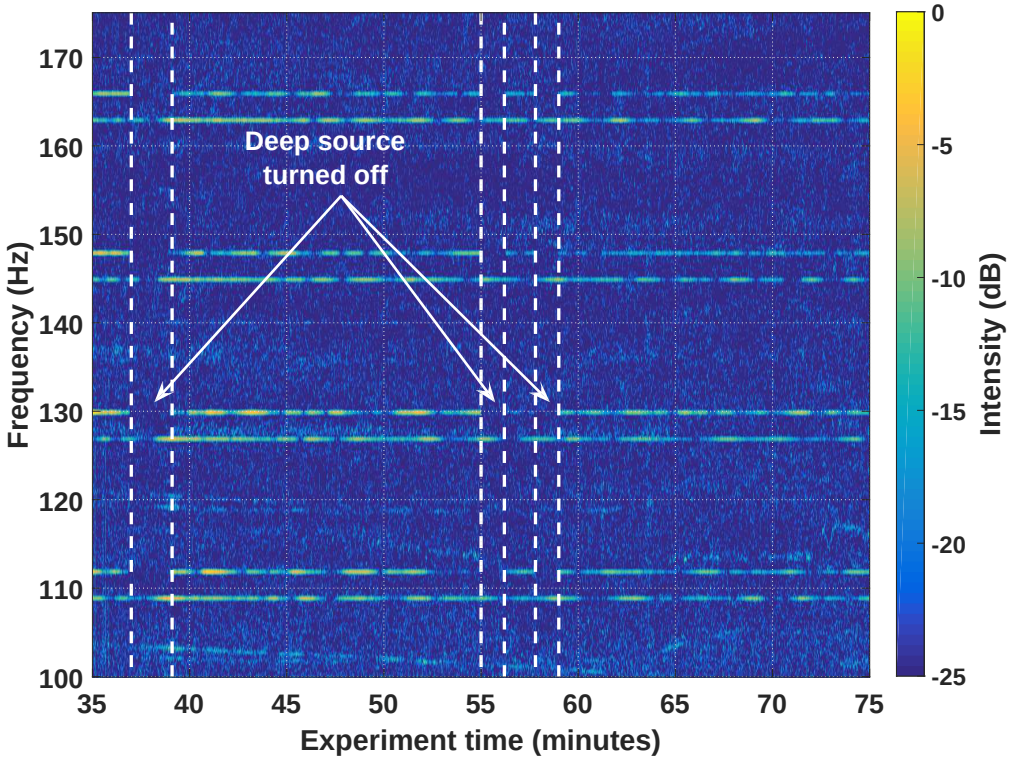

FIGURE 4.2: Spectrogram from Swellex-96 experiment showing 4 pairs of tonals used for processing. The higher frequency tonal in each pair corresponds to the deep source, and the lower frequency tonal corresponds to the shallow source. Note that the deep source was turned off 3 times to transmit FM chirps, as indicated.

event, indicated by the yellow box in Figure 4.1, were selected to use for range-estimation. There were two primary advantages to selecting this portion of the data: first, the source was traveling away from the array at a roughly constant speed over this interval; second, the bathymetry varied by less than 50 meters over this portion of the experimental. As mentioned previously, flat bathymetries are expected to yield better ranging results, as β is known to vary with changes in water column depth at the source location [2].

The acoustic signals transmitted by the shallow and deep sources were separable in the frequency domain, as can be seen from the spectrogram of the data recorded by Hydrophone 1 in Figure 4.2. Note that, although a total of 74 tonals were transmitted

between 49 Hz and 400 Hz, only the 8 tonals shown in Figure 4.2 were selected to be processed. It was desired to select sets of tonals located in the lower frequencies, as cargo ships have been shown to exhibit strong tonal emissions, especially at lower speeds, at low frequecies [7]. Furthermore, it was desired to select tonals with high SNR for experimental purposes, and to select a range of tonals with the smallest ratio of highest frequency to lowest frequency, ω_F/ω_1 as possible to maximize the portion of the $I(r,\omega)$ surface that can be covered by projected striations for range both β and range estimation.

Specifically, the 109, 127, 145, and 163 Hz tonals of the shallow source and the 112, 130, 148, and 166 Hz tonals from the deep source were used. Following the process depicted in the top half of Figure 3.2, the time axis of the spectrogram obtained from hydrophone #1 was converted into a range axis by using GPS data recorded by a receiver located on the tow ship and delayed, as described earlier, to estimate the position of the shallow source. This provided the range-frequency intensity surface $I(r,\omega)$ that is required to find β, which was estimated to be 1.20 when using tonals from the shallow source, and 1.29 when using tonals from the deep source. Over the entire 40 minute observation window, the value of $\hat{\beta}$ computed over any 2km interval, did not deviate from the mean value of 1.20 by more than 0.02, when using the shallow source tonals, even with changes in water column depth of nearly 50 meters. This lends credibility to the notion that a single value of β can adequately describe this channel. Furthermore, for the shallow source, the estimated $\hat{\beta}$ was identical to the value obtained through Kraken simulation. For the deep source, the estimated $\hat{\beta}$ was higher than estimated using the shallow source, as observed through simulation, but in this case the value was higher by 0.09 rather than 0.04 in simulation. Overall, the β estimator exhibits remarkably close agreement between simulated and experimental results.

Once $\hat{\beta}$ was estimated from the shallow source, the range to the deep source was

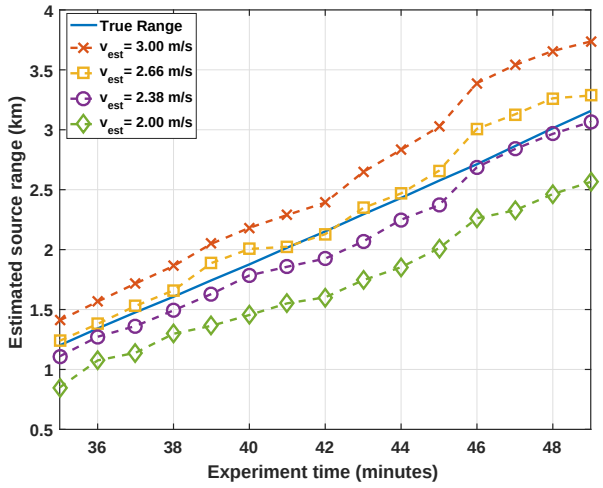

(a) $\hat{\beta} = 1.20$

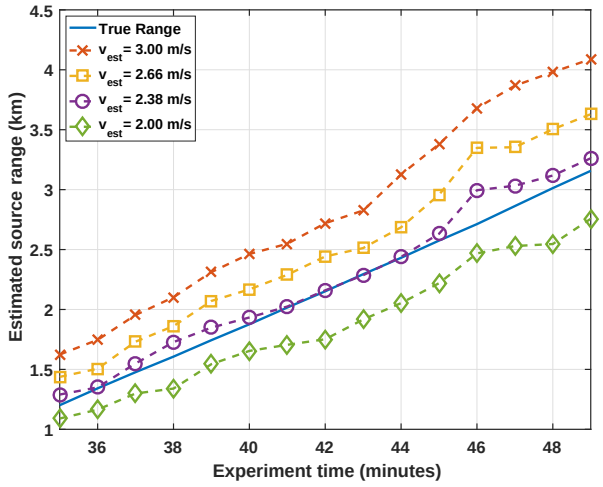

(b) $\hat{\beta} = 1.29$

FIGURE 4.3: Range estimation results obtained from Swellex96 experimental data. Two different estimates of β, obtained from averaging over the entire source track, and four different estimates of source velocity (range rate), are used to estimate the range to the deep source at the beginning of independent, overlapping 20-minute intervals. (a) Range estimates using an estimated $\hat{\beta} = 1.20$ derived from shallow source tonals, (b) Range estimates using $\hat{\beta} = 1.29$ derived from deep source tonals. Note that in (a), the GPS-derived source velocity of 2.38 m/s yields an average ranging error of around -100 meters, while in (b), the same source velocity yields a small positive ranging offset.

estimated in accordance with the procedure depicted in the lower half of Figure 3.2. To provide sufficient data for the estimator to adequately project multiple striations across the range-frequency intensity surface, the 40 minutes of data from hydrophone #1 were broken into 25 overlapping 20-minute windows, with one minute spacing, and the source range was estimated independently in each window. The estimated $\hat{r_0}$ thus corresponds to the range of the deep source at the beginning of a 20-minute data window. Range estimation results are shown in Figure 4.3 for a variety of estimated source velocities $\hat{v}_s = [2.00, 2.38, 2.66, 3.00]$ m/s. Note that source velocity can be estimated using various techniques [16, 18], but the most relevant to this experiment is the cross-correlation source differencing technique proposed by Rakatonarivo and Kuperman [18], as they estimated the source speed for the same data set to be 2.66 m/s. The GPS data indicates the average source velocity over the 40-minute interval of interest was 2.38 m/s. The other values of 2 m/s and 3 m/s are included in Figure 4.3 to examine the impact of incorrect source velocity estimates on range estimation performance.

The GPS-derived $\hat{v}_s$ =2.38 m/s range estimation results indicate an offset of about -100 to -150 meters when using an estimate $\hat{\beta}$ derived from a transiting shallow source to estimate the range to the deep source. This is very close to the -130m offset observed under the same scenario through simulation. Furthermore, when the range estimator is provided the estimate of β corresponding to the deep source, the source range is estimated with nearly zero offset. One peculiarity, which is not shown in Figure 4.3 but deserves some brief mention, is that the source range estimates all drop very sharply around the 50 minute mark. This is caused by the deep source being turned off for about two minutes at both 55 minutes and 57 minutes into the experiment. The projected striations, which start at the lowest-frequency tonal and extend forward in time (increasing range) and upward in frequency, have tonal components that fall into both of the regions where there is no source signal. That

is, the estimated striation intensity, $\hat{I}_{MLE}$, is no longer valid in these regions. In this case, the estimator selects a shorter initial range (equivalently, a higher value of β), favoring projected striations with higher slope that have multiple components in the FM chirp region, where the measured intensity is at the noise floor, matching closely with the intensity of the first tonal, which was located at a null in the channel fading pattern that started at about the 52 minute mark.

With the exception of the aberration in caused by the FM chirps, the performance of the range estimator matches very well with simulation and is also shown to be robust to interference, including complete loss of signal. Furthermore, the standard deviation of the range estimator, given the GPS-derived average source velocity and shallow source estimate of β, up to the 50-minute mark was 65 meters, which compares favorably to the average standard deviation of 55m at 3km source range obtained from 300 Monte Carlo simulations.

5

Conclusions

Two ML-MMSE estimators (β and range to a tonal source) were presented. These estimators are intended to be used in the presence of cargo ships in shallow water environments with slowly-varying bathymetry, while requiring minimal a priori knowledge. At the core of each estimation algorithm is a simple process of projecting isoline "striations" across a range-frequency-intensity $I(r, \omega)$ surface, finding the maximum-likelihood noise-free striation intensity, and then computing the parameter value (β or $\vec{r_0}$) that minimizes the mean squared matching error along the striations. The methods for estimating $\hat{\beta}$ and $\hat{r_0}$ were demonstrated to show excellent agreement between the results of high-fidelity Kraken simulations and real data obtained from the Swellex 96 shallow water experiment, which had slowly-varying bathymetry and well-defined tonal sources. Furthermore, the estimators are shown to be robust against both signal degradation (interfering sources and temporary signal loss) and errors in estimating source velocity. Future work in the area could involve methods for incorporating frequency dependencies into the model of the striation patterns, which could lead to estimators that work well in a wider range of environments while still requiring minimal a priori knowledge of environmental parameters.

Bibliography

[1] S. Chuprov, "Interference structure of a sound field in a layered ocean," *Ocean Acoustics, Current State*, pp. 71–91, 1982.

[2] G. D'Spain and W. A. Kuperman, "Application of waveguide invariants to analysis of spectrograms from shallow water environments that vary in range and azimuth," *Journal of the Acoustical Society of America*, vol. 106, No.5, p. 2454, November 1999.

[3] F. B. Jensen, W. A. Kuperman, M. B. Porter, and H. Schmidt, *Computational Ocean Acoustics*. New York: Springer, 2011.

[4] A. Harms, J. Odom, and J. Krolik, "Ocean acoustic waveguide invariant parameter estimation using tonal noise sources," *ICASSP*, 2015.

[5] D. Rouseff and R. C. Spindel, "Modeling the waveguide invariant as a distribution," *AIP Conference Proceedings*, pp. 137–148, 2002.

[6] A. M. Thode, "Source ranging with minimal environmental information using a virtual receiver and waveguide invariant theory," *The Journal of the Acoustical Society of America*, vol. 108, no. 4, pp. 1582–1594, 2000.

[7] P. T. Arveson and D. J. Vendittis, "Radiated noise characteristics of a modern cargo ship," *The Journal of the Acoustical Society of America*, vol. 107, no. 1, pp. 118–129, 2000.

[8] J. M. Mou, C. V. Tak, and H. Ligteringen, "Study on collision avoidance in busy waterways by using AIS data," *Ocean Engineering*, vol. 37, no. 5-6, pp. 483–490, 2010.

[9] H. M. Perez, R. Chang, R. Billings, and T. L. Kosub, "Automatic Identification Systems (AIS) Data Use in Marine Vessel Emission Estimation," *Time*, no. Cmv, pp. 1–25, 2009.

[10] "United states coast guard navigation center: Nais data sharing categories and requirements." `http://www.navcen.uscg.gov/?pageName=NAISdisclaimer`, 2016. Accessed 2016-02-01.

[11] C. M. Verlinden, J. Sarkar, W. S. Hodgkiss, W. A. Kuperman, and K. G. Sabra, "Passive acoustic source localization using sources of opportunity.," *The Journal of the Acoustical Society of America*, vol. 138, no. 1, pp. EL54–9, 2015.

[12] A. B. Baggeroer, W. A. Kuperman, and P. N. Mikhalevsky, "An overview of matched field methods in ocean acoustics," *IEEE Journal of Oceanic Engineering*, vol. 18, 1993.

[13] M. D. Collins, L. E. Tinker, J. S. Perkins, N. C. Makris, and W. A. Kuperman, "Single-frequency matched-field processing with a single hydrophone," *Journal of the Acoustical Society of America*, vol. 90, 1998.

[14] T. C. Yang, "Beam intensity striations and applications.," *The Journal of the Acoustical Society of America*, vol. 113, no. 3, pp. 1342–1352, 2003.

[15] A. Turgut, M. Orr, and D. Rouseff, "Broadband source localiza- tion using horizontal-beam acoustic intensity striations," *The Journal of the Acoustical Society of America*, vol. 127, pp. 73–83, 2010.

[16] H. Tao, G. Hickman, J. Krolik, and M. Kemp, "Single hydrophone passive localization of transiting acoustic sources," *OCEANS 2007 - Europe*, no. 2, pp. 2–4, 2007.

[17] R. Goldhahn, G. Hickman, and J. Krolik, "Waveguide invariant reverberation mitigation for active sonar," *ICASSP*, vol. 728, pp. 941–944, 2007.

[18] S. Rakotonarivo and W. A. Kuperman, "Model-independent range localization of a moving source in shallow water," *Journal of the Acoustical Society of America*, vol. 132, p. 2218, 2012.

[19] Z. Zhen-dong and W. Hao-zhong, "Broadband Source Ranging in Shallow Water Using the -Interference," vol. 27, no. 6, pp. 1–4, 2010.

[20] K. Cockrell and H. Schmidt, "Robust passive range estimation using the waveguide invariant," *The Journal of the Acoustical Society of America*, vol. 127, pp. 2780–2789, 2010.

[21] P. Wang, L. Zhang, and V. Li, "A Stratified Acoustic Model Accounting for Phase Shifts for Underwater Acoustic Networks," *Sensors*, vol. 13, no. 5, pp. 6183–6203, 2013.

[22] M. Abramowitz and I. Stegun, *Handbook of Mathematical Functions*. Dover Publications, 1972.

[23] S. M. P. Laboratory, "Swellex-96: S5 event." `http://swellex96.ucsd.edu/s5.htm`, 2016. Accessed 2016-01-18.